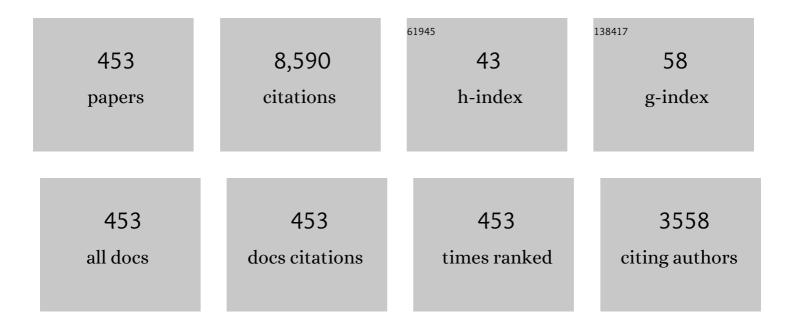
Jose Luis De Pablos

List of Publications by Year in descending order

Source: https://exaly.com/author-pdf/4239161/publications.pdf Version: 2024-02-01



#	Article	IF	CITATIONS
1	Overview of the JET results in support to ITER. Nuclear Fusion, 2017, 57, 102001.	1.6	150
2	ELM divertor peak energy fluence scaling to ITER with data from JET, MAST and ASDEX upgrade. Nuclear Materials and Energy, 2017, 12, 84-90.	0.6	116
3	Isotope effects on L-H threshold and confinement in tokamak plasmas. Plasma Physics and Controlled Fusion, 2018, 60, 014045.	0.9	98
4	Power exhaust by SOL and pedestal radiation at ASDEX Upgrade and JET. Nuclear Materials and Energy, 2017, 12, 111-118.	0.6	92
5	Experimental Validation of a Filament Transport Model in Turbulent Magnetized Plasmas. Physical Review Letters, 2015, 115, 215002.	2.9	89
6	Beryllium migration in JET ITER-like wall plasmas. Nuclear Fusion, 2015, 55, 063021.	1.6	83
7	WEST Physics Basis. Nuclear Fusion, 2015, 55, 063017.	1.6	82
8	Pedestal confinement and stability in JET-ILW ELMy H-modes. Nuclear Fusion, 2015, 55, 113031.	1.6	82
9	Core turbulent transport in tokamak plasmas: bridging theory and experiment with QuaLiKiz. Plasma Physics and Controlled Fusion, 2016, 58, 014036.	0.9	81
10	Improved confinement in JET highβplasmas with an ITER-like wall. Nuclear Fusion, 2015, 55, 053031.	1.6	79
11	Confinement transitions in TJ-II under Li-coated wall conditions. Nuclear Fusion, 2009, 49, 104018.	1.6	75
12	Efficient generation of energetic ions in multi-ion plasmas by radio-frequency heating. Nature Physics, 2017, 13, 973-978.	6.5	73
13	Overview of the JET results with the ITER-like wall. Nuclear Fusion, 2013, 53, 104002.	1.6	70
14	WALLDYN simulations of global impurity migration in JET and extrapolations to ITER. Nuclear Fusion, 2015, 55, 053015.	1.6	67
15	Stationary Zonal Flows during the Formation of the Edge Transport Barrier in the JET Tokamak. Physical Review Letters, 2016, 116, 065002.	2.9	64
16	Dual sightline measurements of MeV range deuterons with neutron and gamma-ray spectroscopy at JET. Nuclear Fusion, 2015, 55, 123026.	1.6	60
17	Runaway electron beam generation and mitigation during disruptions at JET-ILW. Nuclear Fusion, 2015, 55, 093013.	1.6	58
18	Melt damage to the JET ITER-like Wall and divertor. Physica Scripta, 2016, T167, 014070.	1.2	58

#	Article	IF	CITATIONS
19	Erosion and deposition in the JET divertor during the first ILW campaign. Physica Scripta, 2016, T167, 014051.	1.2	58
20	Tractable flux-driven temperature, density, and rotation profile evolution with the quasilinear gyrokinetic transport model QuaLiKiz. Plasma Physics and Controlled Fusion, 2017, 59, 124005.	0.9	57
21	Correlation of the tokamak H-mode density limit with ballooning stability at the separatrix. Nuclear Fusion, 2018, 58, 034001.	1.6	57
22	Key impact of finite-beta and fast ions in core and edge tokamak regions for the transition to advanced scenarios. Nuclear Fusion, 2015, 55, 053007.	1.6	56
23	Influence of theE  ×  Bdrift in high recycling divertors on target asymmetries. Plasma Physics Controlled Fusion, 2015, 57, 095002.	and 0.9	56
24	Recent progress towards a quantitative description of filamentary SOL transport. Nuclear Fusion, 2017, 57, 056044.	1.6	56
25	Internal measurements of Alfvén eigenmodes with heavy ion beam probing in toroidal plasmas*. Nuclear Fusion, 2010, 50, 084023.	1.6	55
26	A new approach to automatic radiation spectrum analysis. IEEE Transactions on Nuclear Science, 1991, 38, 971-975.	1.2	53
27	Direct gyrokinetic comparison of pedestal transport in JET with carbon and ITER-like walls. Nuclear Fusion, 2019, 59, 086056.	1.6	53
28	Long-term fuel retention in JET ITER-like wall. Physica Scripta, 2016, T167, 014075.	1.2	52
29	MeV-range velocity-space tomography from gamma-ray and neutron emission spectrometry measurements at JET. Nuclear Fusion, 2017, 57, 056001.	1.6	52
30	Dust generation in tokamaks: Overview of beryllium and tungsten dust characterisation in JET with the ITER-like wall. Fusion Engineering and Design, 2018, 136, 579-586.	1.0	52
31	First dust study in JET with the ITER-like wall: sampling, analysis and classification. Nuclear Fusion, 2015, 55, 113033.	1.6	51
32	Scaling of the MHD perturbation amplitude required to trigger a disruption and predictions for ITER. Nuclear Fusion, 2016, 56, 026007.	1.6	51
33	Overview of the JET results. Nuclear Fusion, 2015, 55, 104001.	1.6	50
34	The impact of poloidal asymmetries on tungsten transport in the core of JET H-mode plasmas. Physics of Plasmas, 2015, 22, 055902.	0.7	49
35	Plasma potential and turbulence dynamics in toroidal devices (survey of T-10 and TJ-II experiments). Nuclear Fusion, 2011, 51, 083043.	1.6	47
36	A protection system for the JET ITER-like wall based on imaging diagnostics. Review of Scientific Instruments, 2012, 83, 10D727.	0.6	47

#	Article	IF	CITATIONS
37	Progress in understanding disruptions triggered by massive gas injection via 3D non-linear MHD modelling with JOREK. Plasma Physics and Controlled Fusion, 2017, 59, 014006.	0.9	47
38	Overview of fuel inventory in JET with the ITER-like wall. Nuclear Fusion, 2017, 57, 086045.	1.6	47
39	Overview of the JET ITER-like wall divertor. Nuclear Materials and Energy, 2017, 12, 499-505.	0.6	46
40	Scenario development for D–T operation at JET. Nuclear Fusion, 2019, 59, 076037.	1.6	46
41	Three-dimensional non-linear magnetohydrodynamic modeling of massive gas injection triggered disruptions in JET. Physics of Plasmas, 2015, 22, .	0.7	45
42	Beryllium melting and erosion on the upper dump plates in JET during three ITER-like wall campaigns. Nuclear Fusion, 2019, 59, 086009.	1.6	45
43	Plasma Potential Evolution Study by HIBP Diagnostic During NBI Experiments in the TJ-II Stellarator. Fusion Science and Technology, 2007, 51, 31-37.	0.6	44
44	Ion target impact energy during Type I edge localized modes in JET ITER-like Wall. Plasma Physics and Controlled Fusion, 2015, 57, 085006.	0.9	44
45	Heavy ion beam probing—diagnostics to study potential and turbulence in toroidal plasmas. Nuclear Fusion, 2017, 57, 072004.	1.6	44
46	Adaptive predictors based on probabilistic SVM for real time disruption mitigation on JET. Nuclear Fusion, 2018, 58, 056002.	1.6	44
47	Impact of different confinement regimes on the two-dimensional structure of edge turbulence. Plasma Physics and Controlled Fusion, 2006, 48, B465-B473.	0.9	43
48	Real-time control of divertor detachment in H-mode with impurity seeding using Langmuir probe feedback in JET-ITER-like wall. Plasma Physics and Controlled Fusion, 2017, 59, 045001.	0.9	43
49	Role of the pedestal position on the pedestal performance in AUG, JET-ILW and TCV and implications for ITER. Nuclear Fusion, 2019, 59, 076038.	1.6	43
50	First neutron spectroscopy measurements with a pixelated diamond detector at JET. Review of Scientific Instruments, 2016, 87, 11D833.	0.6	42
51	Studies of dust from JET with the ITER-Like Wall: Composition and internal structure. Nuclear Materials and Energy, 2017, 12, 582-587.	0.6	41
52	Real-time-capable prediction of temperature and density profiles in a tokamak using RAPTOR and a first-principle-based transport model. Nuclear Fusion, 2018, 58, 096006.	1.6	41
53	Inferring divertor plasma properties from hydrogen Balmer and Paschen series spectroscopy in JET-ILW. Nuclear Fusion, 2015, 55, 123028.	1.6	40
54	JET and COMPASS asymmetrical disruptions. Nuclear Fusion, 2015, 55, 113006.	1.6	40

#	Article	IF	CITATIONS
55	Integrated modelling of H-mode pedestal and confinement in JET-ILW. Plasma Physics and Controlled Fusion, 2018, 60, 014042.	0.9	40
56	Alfvén eigenmode properties and dynamics in the TJ-II stellarator. Nuclear Fusion, 2012, 52, 123004.	1.6	39
57	Application of Gaussian process regression to plasma turbulent transport model validation via integrated modelling. Nuclear Fusion, 2019, 59, 056007.	1.6	39
58	Overview of JET results. Nuclear Fusion, 2003, 43, 1540-1554.	1.6	38
59	Investigation into the formation of the scrape-off layer density shoulder in JET ITER-like wall L-mode and H-mode plasmas. Nuclear Fusion, 2018, 58, 056001.	1.6	38
60	Effect of the relative shift between the electron density and temperature pedestal position on the pedestal stability in JET-ILW and comparison with JET-C. Nuclear Fusion, 2018, 58, 056010.	1.6	38
61	Overview of TJ-II experiments. Nuclear Fusion, 2005, 45, S266-S275.	1.6	37
62	Physics of Plasmas, 2015, 22, 056115.	0.7	37
63	The role of MHD in causing impurity peaking in JET hybrid plasmas. Nuclear Fusion, 2016, 56, 066002.	1.6	37
64	Multi-machine scaling of the main SOL parallel heat flux width in tokamak limiter plasmas. Plasma Physics and Controlled Fusion, 2016, 58, 074005.	0.9	36
65	Understanding the physics of ELM pacing via vertical kicks in JET in view of ITER. Nuclear Fusion, 2016, 56, 026001.	1.6	36
66	Beryllium global erosion and deposition at JET-ILW simulated with ERO2.0. Nuclear Materials and Energy, 2019, 18, 331-338.	0.6	36
67	Neutron spectroscopy measurements of 14 MeV neutrons at unprecedented energy resolution and implications for deuterium–tritium fusion plasma diagnostics. Measurement Science and Technology, 2018, 29, 045502.	1.4	35
68	Deep learning for plasma tomography using the bolometer system at JET. Fusion Engineering and Design, 2017, 114, 18-25.	1.0	34
69	Dynamics and stability of divertor detachment in H-mode plasmas on JET. Plasma Physics and Controlled Fusion, 2017, 59, 095003.	0.9	34
70	Scenario development for the observation of alpha-driven instabilities in JET DT plasmas. Nuclear Fusion, 2018, 58, 082005.	1.6	34
71	Impact of ICRF on the scrape-off layer and on plasma wall interactions: From present experiments to fusion reactor. Nuclear Materials and Energy, 2019, 18, 131-140.	0.6	34
72	Discriminating the trapped electron modes contribution in density fluctuation spectra. Nuclear Fusion, 2015, 55, 093021.	1.6	33

#	Article	IF	CITATIONS
73	Transport analysis and modelling of the evolution of hollow density profiles plasmas in JET and implication for ITER. Nuclear Fusion, 2015, 55, 123001.	1.6	33
74	Challenges in the extrapolation from DD to DT plasmas: experimental analysis and theory based predictions for JET-DT. Plasma Physics and Controlled Fusion, 2017, 59, 014023.	0.9	33
75	Fast H isotope and impurity mixing in ion-temperature-gradient turbulence. Nuclear Fusion, 2018, 58, 076028.	1.6	33
76	Current Research into Applications of Tomography for Fusion Diagnostics. Journal of Fusion Energy, 2019, 38, 458-466.	0.5	33
77	Effect of magnetic configuration on frequency of NBI-driven Alfvén modes in TJ-II. Nuclear Fusion, 2014, 54, 123002.	1.6	32
78	Ion cyclotron resonance heating for tungsten control in various JET H-mode scenarios. Plasma Physics and Controlled Fusion, 2017, 59, 055001.	0.9	32
79	Experimental estimation of tungsten impurity sputtering due to Type I ELMs in JET-ITER-like wall using pedestal electron cyclotron emission and target Langmuir probe measurements. Physica Scripta, 2016, T167, 014005.	1.2	31
80	Gamma-ray spectroscopy at MHz counting rates with a compact LaBr3 detector and silicon photomultipliers for fusion plasma applications. Review of Scientific Instruments, 2016, 87, 11E714.	0.6	31
81	Fast-ion energy resolution by one-step reaction gamma-ray spectrometry. Nuclear Fusion, 2016, 56, 046009.	1.6	31
82	A First Analysis of JET Plasma Profile-Based Indicators for Disruption Prediction and Avoidance. IEEE Transactions on Plasma Science, 2018, 46, 2691-2698.	0.6	31
83	Isotope identity experiments in JET-ILW with H and D L-mode plasmas. Nuclear Fusion, 2019, 59, 076028.	1.6	31
84	Development of equatorial visible/infrared wide angle viewing system and radial neutron camera for ITER. Fusion Engineering and Design, 2009, 84, 1689-1696.	1.0	30
85	Velocity-space sensitivities of neutron emission spectrometers at the tokamaks JET and ASDEX Upgrade in deuterium plasmas. Review of Scientific Instruments, 2017, 88, 073506.	0.6	30
86	Studies of the pedestal structure and inter-ELM pedestal evolution in JET with the ITER-like wall. Nuclear Fusion, 2017, 57, 116012.	1.6	30
87	Benchmark experiments on neutron streaming through JET Torus Hall penetrations. Nuclear Fusion, 2015, 55, 053028.	1.6	29
88	Axisymmetric oscillations at Lâ \in "H transitions in JET: M-mode. Nuclear Fusion, 2017, 57, 022021.	1.6	29
89	Non-Maxwellian fast particle effects in gyrokinetic GENE simulations. Physics of Plasmas, 2018, 25, .	0.7	29
90	3D non-linear MHD simulation of the MHD response and density increase as a result of shattered pellet injection. Nuclear Fusion, 2018, 58, 126025.	1.6	29

#	Article	IF	CITATIONS
91	Modelling of JET hybrid plasmas with emphasis on performance of combined ICRF and NBI heating. Nuclear Fusion, 2018, 58, 106037.	1.6	29
92	Plasma confinement at JET. Plasma Physics and Controlled Fusion, 2016, 58, 014034.	0.9	28
93	Assessment of erosion, deposition and fuel retention in the JET-ILW divertor from ion beam analysis data. Nuclear Materials and Energy, 2017, 12, 559-563.	0.6	28
94	Sheared flows and turbulence in fusion plasmas. Plasma Physics and Controlled Fusion, 2007, 49, B303-B311.	0.9	27
95	Characterisation of the deuterium recycling at the W divertor target plates in JET during steady-state plasma conditions and ELMs. Physica Scripta, 2016, T167, 014076.	1.2	27
96	Gyrokinetic study of turbulent convection of heavy impurities in tokamak plasmas at comparable ion and electron heat fluxes. Nuclear Fusion, 2017, 57, 022009.	1.6	27
97	Assessment of SOLPS5.0 divertor solutions with drifts and currents against L-mode experiments in ASDEX Upgrade and JET. Plasma Physics and Controlled Fusion, 2017, 59, 035003.	0.9	27
98	First ERO2.0 modeling of Be erosion and non-local transport in JET ITER-like wall. Physica Scripta, 2017, T170, 014018.	1.2	27
99	Erosion and deposition in the JET divertor during the second ITER-like wall campaign. Physica Scripta, 2017, T170, 014058.	1.2	27
100	An Analytical Expression for the Electric Field and Particle Tracing in Modelling of Be Erosion Experiments at the JET ITERâ€like Wall. Contributions To Plasma Physics, 2016, 56, 640-645.	0.5	26
101	Technological exploitation of Deuterium–Tritium operations at JET in support of ITER design, operation and safety. Fusion Engineering and Design, 2016, 109-111, 278-285.	1.0	26
102	Experience on divertor fuel retention after two ITER-Like Wall campaigns. Physica Scripta, 2017, T170, 014063.	1.2	26
103	Dimensionless scalings of confinement, heat transport and pedestal stability in JET-ILW and comparison with JET-C. Plasma Physics and Controlled Fusion, 2017, 59, 014014.	0.9	26
104	Test particles dynamics in the JOREK 3D non-linear MHD code and application to electron transport in a disruption simulation. Nuclear Fusion, 2018, 58, 016043.	1.6	26
105	Assessment of the baseline scenario at <i>q</i> ₉₅ ~ 3 for ITER. Nuclear Fusion, 2018, 58, 126010.	1.6	26
106	W transport and accumulation control in the termination phase of JET H-mode discharges and implications for ITER. Plasma Physics and Controlled Fusion, 2018, 60, 074008.	0.9	26
107	Runaway electron beam control. Plasma Physics and Controlled Fusion, 2019, 61, 014036.	0.9	26
108	Physics of sheared flow development in the boundary of fusion plasmas. Plasma Physics and Controlled Fusion, 2006, 48, S169-S176.	0.9	25

#	Article	IF	CITATIONS
109	Fast ion energy distribution from third harmonic radio frequency heating measured with a single crystal diamond detector at the Joint European Torus. Review of Scientific Instruments, 2015, 86, 103501.	0.6	25
110	Impact of divertor geometry on radiative divertor performance in JET H-mode plasmas. Plasma Physics and Controlled Fusion, 2016, 58, 045011.	0.9	25
111	Plasma impact on diagnostic mirrors in JET. Nuclear Materials and Energy, 2017, 12, 506-512.	0.6	25
112	Recent progress in the quantitative validation of JOREK simulations of ELMs in JET. Nuclear Fusion, 2017, 57, 076006.	1.6	25
113	Fuel inventory and deposition in castellated structures in JET-ILW. Nuclear Fusion, 2017, 57, 066027.	1.6	25
114	Long-term fuel retention and release in JET ITER-Like Wall at ITER-relevant baking temperatures. Nuclear Fusion, 2017, 57, 086024.	1.6	25
115	Maximum likelihood bolometric tomography for the determination of the uncertainties in the radiation emission on JET TOKAMAK. Review of Scientific Instruments, 2018, 89, 053504.	0.6	25
116	Material migration and fuel retention studies during the JET carbon divertor campaigns. Fusion Engineering and Design, 2019, 138, 78-108.	1.0	25
117	The â€~neutron deficit' in the JET tokamak. Nuclear Fusion, 2017, 57, 076029.	1.6	25
118	Overview of TJ-II experiments. Nuclear Fusion, 2011, 51, 094022.	1.6	24
119	The ITER Equatorial Visible/Infra-Red Wide Angle Viewing System: Status of design and R&D. Fusion Engineering and Design, 2015, 96-97, 932-937.	1.0	24
120	Performance of the prototype LaBr3 spectrometer developed for the JET gamma-ray camera upgrade. Review of Scientific Instruments, 2016, 87, 11E717.	0.6	24
121	Experimental investigation of geodesic acoustic modes on JET using Doppler backscattering. Nuclear Fusion, 2016, 56, 106026.	1.6	24
122	Impact of divertor geometry on H-mode confinement in the JET metallic wall. Nuclear Fusion, 2017, 57, 086025.	1.6	24
123	Modelling of tungsten erosion and deposition in the divertor of JET-ILW in comparison to experimental findings. Nuclear Materials and Energy, 2019, 18, 239-244.	0.6	24
124	First mirror test in JET for ITER: Complete overview after three ILW campaigns. Nuclear Materials and Energy, 2019, 19, 59-66.	0.6	24
125	Asymmetric toroidal eddy currents (ATEC) to explain sideways forces at JET. Nuclear Fusion, 2016, 56, 106010.	1.6	23
126	Sawtooth pacing with on-axis ICRH modulation in JET-ILW. Nuclear Fusion, 2017, 57, 036027.	1.6	23

#	Article	IF	CITATIONS
127	High fusion performance at high <i>T</i> _i / <i>T</i> _e in JET-ILW baseline plasmas with high NBI heating power and low gas puffing. Nuclear Fusion, 2018, 58, 036020.	1.6	23
128	Instrumentation for the upgrade to the JET core charge-exchange spectrometers. Review of Scientific Instruments, 2018, 89, 10D113.	0.6	23
129	Impact of electron-scale turbulence and multi-scale interactions in the JET tokamak. Nuclear Fusion, 2018, 58, 124003.	1.6	23
130	ECRH effect on the electric potential and turbulence in the TJ-II stellarator and T-10 tokamak plasmas. Plasma Physics and Controlled Fusion, 2018, 60, 084008.	0.9	23
131	Measuring fast ions in fusion plasmas with neutron diagnostics at JET. Plasma Physics and Controlled Fusion, 2019, 61, 014027.	0.9	23
132	Determination of isotope ratio in the divertor of JET-ILW by high-resolution H <i>α</i> spectroscopy: H–D experiment and implications for D–T experiment. Nuclear Fusion, 2019, 59, 046011.	1.6	23
133	Deposition of impurity metals during campaigns with the JET ITER-like Wall. Nuclear Materials and Energy, 2019, 19, 218-224.	0.6	23
134	Determination of tungsten and molybdenum concentrations from an x-ray range spectrum in JET with the ITER-like wall configuration. Journal of Physics B: Atomic, Molecular and Optical Physics, 2015, 48, 144023.	0.6	22
135	Gyrokinetic study of turbulence suppression in a JET-ILW power scan. Plasma Physics and Controlled Fusion, 2016, 58, 115005.	0.9	22
136	Neutron emission spectroscopy of DT plasmas at enhanced energy resolution with diamond detectors. Review of Scientific Instruments, 2016, 87, 11D822.	0.6	22
137	Global and pedestal confinement and pedestal structure in dimensionless collisionality scans of low-triangularity H-mode plasmas in JET-ILW. Nuclear Fusion, 2017, 57, 016012.	1.6	22
138	Modelling of transitions between L- and H-mode in JET high plasma current plasmas and application to ITER scenarios including tungsten behaviour. Nuclear Fusion, 2017, 57, 086023.	1.6	22
139	Fine metal dust particles on the wall probes from JET-ILW. Physica Scripta, 2017, T170, 014038.	1.2	22
140	Full-Pulse Tomographic Reconstruction with Deep Neural Networks. Fusion Science and Technology, 2018, 74, 47-56.	0.6	22
141	14 MeV calibration of JET neutron detectors—phase 1: calibration and characterization of the neutron source. Nuclear Fusion, 2018, 58, 026012.	1.6	22
142	First principles of modelling the stabilization of microturbulence by fast ions. Nuclear Fusion, 2018, 58, 082024.	1.6	22
143	First principle integrated modeling of multi-channel transport including Tungsten in JET. Nuclear Fusion, 2018, 58, 096003.	1.6	22
144	Radiation asymmetries during the thermal quench of massive gas injection disruptions in JET. Nuclear Fusion, 2015, 55, 123027.	1.6	21

#	Article	IF	CITATIONS
145	Experimental evaluation of stable long term operation of semiconductor magnetic sensors at ITER relevant environment. Nuclear Fusion, 2015, 55, 083006.	1.6	21
146	The upgraded JET gamma-ray cameras based on high resolution/high count rate compact spectrometers. Review of Scientific Instruments, 2018, 89, 101116.	0.6	21
147	Electron acceleration in a JET disruption simulation. Nuclear Fusion, 2018, 58, 106022.	1.6	21
148	Electron internal transport barriers, rationals and quasi-coherent oscillations in the stellarator TJ-II. Plasma Physics and Controlled Fusion, 2005, 47, L57-L63.	0.9	20
149	Spatially resolved Hα-emission simulation with EIRENE in TJ-II to study hydrogen atomic and molecular physics in low density, high temperature fusion edge plasmas. Nuclear Fusion, 2008, 48, 095005.	1.6	20
150	Non-linear MHD simulations of ELMs in JET and quantitative comparisons to experiments. Plasma Physics and Controlled Fusion, 2016, 58, 014026.	0.9	20
151	Deuterium trapping and release in JET ITER-like wall divertor tiles. Physica Scripta, 2016, T167, 014074.	1.2	20
152	ITER oriented neutronics benchmark experiments on neutron streaming and shutdown dose rate at JET. Fusion Engineering and Design, 2017, 123, 171-176.	1.0	20
153	Simulation of neutral gas flow in the JET sub-divertor. Fusion Engineering and Design, 2017, 121, 13-21.	1.0	20
154	Transient induced tungsten melting at the Joint European Torus (JET). Physica Scripta, 2017, T170, 014013.	1.2	20
155	Multi-machine analysis of termination scenarios with comparison to simulations of controlled shutdown of ITER discharges. Nuclear Fusion, 2018, 58, 026019.	1.6	20
156	Experimental validation of an analytical kinetic model for edge-localized modes in JET-ITER-like wall. Nuclear Fusion, 2018, 58, 066006.	1.6	20
157	Identification of BeO and BeOxDy in melted zones of the JET Be limiter tiles: Raman study using comparison with laboratory samples. Nuclear Materials and Energy, 2018, 17, 295-301.	0.6	20
158	Tritium retention characteristics in dust particles in JET with ITER-like wall. Nuclear Materials and Energy, 2018, 17, 279-283.	0.6	20
159	Equilibrium reconstruction at JET using Stokes model for polarimetry. Nuclear Fusion, 2018, 58, 106032.	1.6	20
160	Observation of enhanced ion particle transport in mixed H/D isotope plasmas on JET. Nuclear Fusion, 2018, 58, 076022.	1.6	20
161	14 MeV calibration of JET neutron detectors—phase 2: in-vessel calibration. Nuclear Fusion, 2018, 58, 106016.	1.6	20
162	Progress of the ITER equatorial vis/IR wide angle viewing system optical design. Review of Scientific Instruments, 2008, 79, 10F509.	0.6	19

#	Article	IF	CITATIONS
163	Changes in plasma potential and turbulent particle flux in the core plasma measured by heavy ion beam probe during L–H transitions in the TJ-II stellarator. Nuclear Fusion, 2013, 53, 092002.	1.6	19
164	Neutronics experiments and analyses in preparation of DT operations at JET. Fusion Engineering and Design, 2016, 109-111, 895-905.	1.0	19
165	JET experiments with tritium and deuterium–tritium mixtures. Fusion Engineering and Design, 2016, 109-111, 925-936.	1.0	19
166	Impact of toroidal and poloidal mode spectra on the control of non-axisymmetric fields in tokamaks. Physics of Plasmas, 2017, 24, .	0.7	19
167	Mitigation of divertor heat loads by strike point sweeping in high power JET discharges. Physica Scripta, 2017, T170, 014040.	1.2	19
168	Neutral pathways and heat flux widths in vertical- and horizontal-target EDGE2D-EIRENE simulations of JET. Nuclear Fusion, 2018, 58, 096029.	1.6	19
169	Thermal desorption spectrometry of beryllium plasma facing tiles exposed in the JET tokamak. Fusion Engineering and Design, 2018, 133, 135-141.	1.0	19
170	L to H mode transition: parametric dependencies of the temperature threshold. Nuclear Fusion, 2015, 55, 073015.	1.6	18
171	High performance detectors for upgraded gamma ray diagnostics for JET DT campaigns. Physica Scripta, 2016, 91, 064003.	1.2	18
172	Response function of single crystal synthetic diamond detectors to 1-4 MeV neutrons for spectroscopy of D plasmas. Review of Scientific Instruments, 2016, 87, 11D823.	0.6	18
173	Nitrogen retention mechanisms in tokamaks with beryllium and tungsten plasma-facing surfaces. Physica Scripta, 2016, T167, 014077.	1.2	18
174	Experience of handling beryllium, tritium and activated components from JET ITER like wall. Physica Scripta, 2016, T167, 014057.	1.2	18
175	The role and application of ion beam analysis for studies of plasma-facing components in controlled fusion devices. Nuclear Instruments & Methods in Physics Research B, 2016, 371, 4-11.	0.6	18
176	Application of transfer entropy to causality detection and synchronization experiments in tokamaks. Nuclear Fusion, 2016, 56, 026006.	1.6	18
177	Energy balance in JET. Nuclear Materials and Energy, 2017, 12, 227-233.	0.6	18
178	A multi-machine scaling of halo current rotation. Nuclear Fusion, 2018, 58, 016050.	1.6	18
179	Investigation of deuterium trapping and release in the JET ITER-like wall divertor using TDS and TMAP. Nuclear Materials and Energy, 2019, 19, 166-178.	0.6	18
180	Analysis of deposited layers with deuterium and impurity elements on samples from the divertor of JET with ITER-like wall. Journal of Nuclear Materials, 2019, 516, 202-213.	1.3	18

#	Article	IF	CITATIONS
181	Benchmarking the GENE and GYRO codes through the relative roles of electromagnetic and <i>E</i> × <i>B</i> stabilization in JET high-performance discharges. Plasma Physics and G Fusion, 2016, 58, 125018.	Controlled	17
182	Improved ERO modelling for spectroscopy of physically and chemically assisted eroded beryllium from the JET-ILW. Nuclear Materials and Energy, 2016, 9, 604-609.	0.6	17
183	Investigation and plasma cleaning of first mirrors coated with relevant ITER contaminants: beryllium and tungsten. Nuclear Fusion, 2017, 57, 086019.	1.6	17
184	Calibration of neutron detectors on the Joint European Torus. Review of Scientific Instruments, 2017, 88, 103505.	0.6	17
185	Versatile fusion source integrator AFSI for fast ion and neutron studies in fusion devices. Nuclear Fusion, 2018, 58, 016023.	1.6	17
186	High-resolution tungsten spectroscopy relevant to the diagnostic of high-temperature tokamak plasmas. Physical Review A, 2018, 97, .	1.0	17
187	Analysis of ELM stability with extended MHD models in JET, JT-60U and future JT-60SA tokamak plasmas. Plasma Physics and Controlled Fusion, 2018, 60, 014032.	0.9	17
188	Effects of nitrogen seeding on core ion thermal transport in JET ILW L-mode plasmas. Nuclear Fusion, 2018, 58, 026028.	1.6	17
189	Synthetic spectra of BeH, BeD and BeT for emission modeling in JET plasmas. Journal of Physics B: Atomic, Molecular and Optical Physics, 2018, 51, 185701.	0.6	17
190	Activation of ITER materials in JET: nuclear characterisation experiments for the long-term irradiation station. Nuclear Fusion, 2018, 58, 096013.	1.6	17
191	Heavy ion beam probe design and operation on the T-10 tokamak. Fusion Engineering and Design, 2019, 146, 850-853.	1.0	17
192	Detecting non-Maxwellian electron velocity distributions at JET by high resolution Thomson scattering. Review of Scientific Instruments, 2011, 82, 033514.	0.6	16
193	Control and data acquisition for dual HIBP diagnostics in the TJ-II stellarator. Fusion Engineering and Design, 2015, 96-97, 724-728.	1.0	16
194	Transition from chirping to steady NBI-driven Alfvén modes caused by magnetic configuration variations in the TJ-II stellarator. Nuclear Fusion, 2016, 56, 076001.	1.6	16
195	Possible influence of near SOL plasma on the H-mode power threshold. Nuclear Materials and Energy, 2017, 12, 273-277.	0.6	16
196	Axisymmetric global Alfvén eigenmodes within the ellipticity-induced frequency gap in the Joint European Torus. Physics of Plasmas, 2017, 24, .	0.7	16
197	Bayesian electron density inference from JET lithium beam emission spectra using Gaussian processes. Nuclear Fusion, 2017, 57, 036017.	1.6	16
198	3D effects on transport and plasma control in the TJ-II stellarator. Nuclear Fusion, 2017, 57, 102022.	1.6	16

#	Article	IF	CITATIONS
199	Dependence of the turbulent particle flux on hydrogen isotopes induced by collisionality. Physics of Plasmas, 2018, 25, 082517.	0.7	16
200	Density profile reconstruction using HIBP in ECRH plasmas in the TJ-II stellarator. Journal of Instrumentation, 2019, 14, C09033-C09033.	0.5	16
201	Determination of tungsten sources in the JET-ILW divertor by spectroscopic imaging in the presence of a strong plasma continuum. Nuclear Materials and Energy, 2019, 18, 118-124.	0.6	16
202	Study of NBI-driven chirping mode properties and radial location by the heavy ion beam probe in the TJ-II stellarator. Nuclear Fusion, 2016, 56, 112019.	1.6	15
203	Bayesian Integrated Data Analysis of Fast-Ion Measurements by Velocity-Space Tomography. Fusion Science and Technology, 2018, 74, 23-36.	0.6	15
204	Correlation of surface chemical states with hydrogen isotope retention in divertor tiles of JET with ITER-Like Wall. Fusion Engineering and Design, 2018, 132, 24-28.	1.0	15
205	Improved ERO modelling of beryllium erosion at ITER upper first wall panel using JET-ILW and PISCES-B experience. Nuclear Materials and Energy, 2019, 19, 510-515.	0.6	15
206	The effect of beryllium oxide on retention in JET ITER-like wall tiles. Nuclear Materials and Energy, 2019, 19, 346-351.	0.6	15
207	Fast ion synergistic effects in JET high performance pulses. Nuclear Fusion, 2019, 59, 056005.	1.6	15
208	Deep deuterium retention and Be/W mixing at tungsten coated surfaces in the JET divertor. Physica Scripta, 2016, T167, 014061.	1.2	14
209	How to assess the efficiency of synchronization experiments in tokamaks. Nuclear Fusion, 2016, 56, 076008.	1.6	14
210	Deposition in the inner and outer corners of the JET divertor with carbon wall and metallic ITER-like wall. Physica Scripta, 2016, T167, 014052.	1.2	14
211	Raman microscopy investigation of beryllium materials. Physica Scripta, 2016, T167, 014027.	1.2	14
212	Beryllium film deposition in cavity samples in remote areas of the JET divertor during the 2011–2012 ITER-like wall campaign. Nuclear Materials and Energy, 2017, 12, 548-552.	0.6	14
213	Micro-/nano-characterization of the surface structures on the divertor tiles from JET ITER-like wall. Fusion Engineering and Design, 2017, 116, 1-4.	1.0	14
214	Structure, tritium depth profile and desorption from â€~plasma-facing' beryllium materials of ITER-Like-Wall at JET. Nuclear Materials and Energy, 2017, 12, 642-647.	0.6	14
215	3D simulations of gas puff effects on edge plasma and ICRF coupling in JET. Nuclear Fusion, 2017, 57, 056042.	1.6	14
216	Sub-millisecond electron density profile measurement at the JET tokamak with the fast lithium beam emission spectroscopy system. Review of Scientific Instruments, 2018, 89, 043509.	0.6	14

#	Article	IF	CITATIONS
217	High Z neoclassical transport: Application and limitation of analytical formulae for modelling JET experimental parameters. Physics of Plasmas, 2018, 25, .	0.7	14
218	Pedestal evolution physics in low triangularity JET tokamak discharges with ITER-like wall. Nuclear Fusion, 2018, 58, 016021.	1.6	14
219	On the Use of Transfer Entropy to Investigate the Time Horizon of Causal Influences between Signals. Entropy, 2018, 20, 627.	1.1	14
220	Real-time protection of the JET ITER-like wall based on near infrared imaging diagnostic systems. Nuclear Fusion, 2018, 58, 106021.	1.6	14
221	Observations and modelling of ion cyclotron emission observed in JET plasmas using a sub-harmonic arc detection system during ion cyclotron resonance heating. Nuclear Fusion, 2018, 58, 096020.	1.6	14
222	Total and elastic electron scattering cross sections from ozone at intermediate and high energies. Journal of Physics B: Atomic, Molecular and Optical Physics, 2002, 35, 865-874.	0.6	13
223	Electron Internal Transport Barriers and Magnetic Topology in the Stellarator TJ-II. Fusion Science and Technology, 2006, 50, 127-135.	0.6	13
224	Radiation damage and nuclear heating studies in selected functional materials during the JET DT campaign. Fusion Engineering and Design, 2016, 109-111, 1011-1015.	1.0	13
225	High power neon seeded JET discharges: Experiments and simulations. Nuclear Materials and Energy, 2017, 12, 882-886.	0.6	13
226	Surface composition and structure of divertor tiles following the JET tokamak operation with the ITER-like wall. Nuclear Fusion, 2017, 57, 076027.	1.6	13
227	Deuterium retention in the divertor tiles of JET ITER-Like wall. Nuclear Materials and Energy, 2017, 12, 655-661.	0.6	13
228	Analyses of microstructure, composition and retention of hydrogen isotopes in divertor tiles of JET with the ITER-like wall. Physica Scripta, 2017, T170, 014031.	1.2	13
229	Light impurity transport in JET ILW L-mode plasmas. Nuclear Fusion, 2018, 58, 036009.	1.6	13
230	Determination of 2D poloidal maps of the intrinsic W density for transport studies in JET-ILW. Review of Scientific Instruments, 2018, 89, 113501.	0.6	13
231	Gyrokinetic modeling of impurity peaking in JET H-mode plasmas. Physics of Plasmas, 2017, 24, .	0.7	13
232	Trapped electron mode driven electron heat transport in JET: experimental investigation and gyro-kinetic theory validation. Nuclear Fusion, 2015, 55, 113016.	1.6	12
233	Diagnostic application of magnetic islands rotation in JET. Nuclear Fusion, 2016, 56, 076004.	1.6	12
234	Studies of Be migration in the JET tokamak using AMS with 10Be marker. Nuclear Instruments & Methods in Physics Research B, 2016, 371, 370-375.	0.6	12

#	Article	IF	CITATIONS
235	Calculations to support JET neutron yield calibration: Modelling of neutron emission from a compact DT neutron generator. Nuclear Instruments and Methods in Physics Research, Section A: Accelerators, Spectrometers, Detectors and Associated Equipment, 2017, 847, 199-204.	0.7	12
236	A tool to support the construction of reliable disruption databases. Fusion Engineering and Design, 2017, 125, 139-153.	1.0	12
237	Erosion at the inner wall of JET during the discharge campaign 2013–2014. Nuclear Materials and Energy, 2017, 11, 20-24.	0.6	12
238	Assessment of divertor heat load with and without external magnetic perturbation. Nuclear Fusion, 2017, 57, 066045.	1.6	12
239	Metallic mirrors for plasma diagnosis in current and future reactors: tests for ITER and DEMO. Physica Scripta, 2017, T170, 014061.	1.2	12
240	Equilibrium reconstruction in an iron core tokamak using a deterministic magnetisation model. Computer Physics Communications, 2018, 223, 1-17.	3.0	12
241	Comparison of runaway electron generation parameters in small, medium-sized and large tokamaks—A survey of experiments in COMPASS, TCV, ASDEX-Upgrade and JET. Nuclear Fusion, 2018, 58, 016014.	1.6	12
242	Assessment of the strength of kinetic effects of parallel electron transport in the SOL and divertor of JET high radiative H-mode plasmas using EDGE2D-EIRENE and KIPP codes. Plasma Physics and Controlled Fusion, 2018, 60, 115011.	0.9	12
243	Development of a new compact gamma-ray spectrometer optimised for runaway electron measurements. Review of Scientific Instruments, 2018, 89, 10I134.	0.6	12
244	Overview of recent TJ-II stellarator results. Nuclear Fusion, 2019, 59, 112019.	1.6	12
245	Dynamic modelling of local fuel inventory and desorption in the whole tokamak vacuum vessel for auto-consistent plasma-wall interaction simulations. Nuclear Materials and Energy, 2019, 19, 550-557.	0.6	12
246	Diagnostic of fast-ion energy spectra and densities in magnetized plasmas. Journal of Instrumentation, 2019, 14, C05019-C05019.	0.5	12
247	The dynamics of the formation of the edge particle transport barrier at TJ-II. Nuclear Fusion, 2011, 51, 113002.	1.6	11
248	On the interpretation of high-resolution x-ray spectra from JET with an ITER-like wall. Journal of Physics B: Atomic, Molecular and Optical Physics, 2015, 48, 144028.	0.6	11
249	Neutron streaming along ducts and labyrinths at the JET biological shielding: Effect of concrete composition. Radiation Physics and Chemistry, 2015, 116, 359-364.	1.4	11
250	Progress in reducing ICRF-specific impurity release in ASDEX upgrade and JET. Nuclear Materials and Energy, 2017, 12, 1194-1198.	0.6	11
251	Upgrade of the tangential gamma-ray spectrometer beam-line for JET DT experiments. Fusion Engineering and Design, 2017, 123, 749-753.	1.0	11
252	Numerical analysis of ELM stability with rotation and ion diamagnetic drift effects in JET. Nuclear Fusion, 2017, 57, 126001.	1.6	11

#	Article	IF	CITATIONS
253	Activation measurements in support of the 14 MeV neutron calibration of JET neutron monitors. Fusion Engineering and Design, 2017, 125, 50-56.	1.0	11
254	Statistical validation of predictive TRANSP simulations of baseline discharges in preparation for extrapolation to JET D–T. Nuclear Fusion, 2017, 57, 066032.	1.6	11
255	Comparison of JET AVDE disruption data with M3D simulations and implications for ITER. Physics of Plasmas, 2017, 24, .	0.7	11
256	TAE stability calculations compared to TAE antenna results in JET. Nuclear Fusion, 2018, 58, 082007.	1.6	11
257	EDGE2D-EIRENE simulations of the influence of isotope effects and anomalous transport coefficients on near scrape-off layer radial electric field. Plasma Physics and Controlled Fusion, 2019, 61, 075010.	0.9	11
258	Investigation of deuterium trapping and release in the JET divertor during the third ILW campaign using TDS. Nuclear Materials and Energy, 2019, 19, 300-306.	0.6	11
259	Long-lived coupled peeling ballooning modes preceding ELMs on JET. Nuclear Fusion, 2019, 59, 056004.	1.6	11
260	Total and elastic electron scattering cross sections from Xe at intermediate and high energies. Journal of Physics B: Atomic, Molecular and Optical Physics, 2002, 35, 4657-4667.	0.6	10
261	An FPGA-based bolometer for the MAST-U Super-X divertor. Review of Scientific Instruments, 2016, 87, 11E721.	0.6	10
262	Bayesian modelling of the emission spectrum of the Joint European Torus Lithium Beam Emission Spectroscopy system. Review of Scientific Instruments, 2016, 87, 023501.	0.6	10
263	Extending helium partial pressure measurement technology to JET DTE2 and ITER. Review of Scientific Instruments, 2016, 87, 11D442.	0.6	10
264	Advanced design of the Mechanical Tritium Pumping System for JET DTE2. Fusion Engineering and Design, 2016, 109-111, 359-364.	1.0	10
265	Tritium distributions on tungsten and carbon tiles used in the JET divertor. Physica Scripta, 2016, T167, 014009.	1.2	10
266	In situ wavelength calibration of the edge CXS spectrometers on JET. Review of Scientific Instruments, 2016, 87, 11E525.	0.6	10
267	Technical preparations for the in-vessel 14 MeV neutron calibration at JET. Fusion Engineering and Design, 2017, 117, 107-114.	1.0	10
268	Status of ITER material activation experiments at JET. Fusion Engineering and Design, 2017, 124, 1150-1155.	1.0	10
269	On efficiency and interpretation of sawteeth pacing with on-axis ICRH modulation in JET. Nuclear Fusion, 2017, 57, 126057.	1.6	10
270	Simulation of JET ITER-Like Wall pulses at high neon seeding rate. Nuclear Fusion, 2017, 57, 126021.	1.6	10

#	Article	IF	CITATIONS
271	The isotope effect on divertor conditions and neutral pumping in horizontal divertor configurations in JET-ILW Ohmic plasmas. Nuclear Materials and Energy, 2017, 12, 791-797.	0.6	10
272	An analytical expression for ion velocities at the wall including the sheath electric field and surface biasing for erosion modeling at JET ILW. Nuclear Materials and Energy, 2017, 12, 341-345.	0.6	10
273	On the potential of ruled-based machine learning for disruption prediction on JET. Fusion Engineering and Design, 2018, 130, 62-68.	1.0	10
274	Tritium distributions on W-coated divertor tiles used in the third JET ITER-like wall campaign. Nuclear Materials and Energy, 2019, 18, 258-261.	0.6	10
275	Overview of TJ-II experiments. Nuclear Fusion, 2007, 47, S677-S685.	1.6	9
276	On the operational specifications and associated R&D for the VIS/IR diagnostic for ITER. , 2009, , .		9
277	Double imaging with an intensified visible fast camera to visualize the fine structure of turbulent coherent plasma structures (blobs) in TJ-II. Plasma Physics and Controlled Fusion, 2014, 56, 105003.	0.9	9
278	Transport, stability and plasma control studies in the TJ-II stellarator. Nuclear Fusion, 2015, 55, 104014.	1.6	9
279	Study of the triton-burnup process in different JET scenarios using neutron monitor based on CVD diamond. Review of Scientific Instruments, 2016, 87, 11D835.	0.6	9
280	JET diagnostic enhancements in preparation for DT operations. Review of Scientific Instruments, 2016, 87, 11D443.	0.6	9
281	Hardware architecture of the data acquisition and processing system for the JET Neutron Camera Upgrade (NCU) project. Fusion Engineering and Design, 2017, 123, 873-876.	1.0	9
282	The effect of the isotope on the H-mode density limit. Nuclear Fusion, 2017, 57, 086007.	1.6	9
283	The emissivity of W coatings deposited on carbon materials for fusion applications. Fusion Engineering and Design, 2017, 114, 192-195.	1.0	9
284	A system of containment to prevent oil spills from sunken tankers. Science of the Total Environment, 2017, 593-594, 242-252.	3.9	9
285	Response of the imaging cameras to hard radiation during JET operation. Fusion Engineering and Design, 2017, 123, 669-673.	1.0	9
286	ERO modeling and sensitivity analysis of locally enhanced beryllium erosion by magnetically connected antennas. Nuclear Fusion, 2018, 58, 016046.	1.6	9
287	Modelling of the neutron production in a mixed beam DT neutron generator. Fusion Engineering and Design, 2018, 136, 1089-1093.	1.0	9
288	Generation of a plasma neutron source for Monte Carlo neutron transport calculations in the tokamak JET. Fusion Engineering and Design, 2018, 136, 1047-1051.	1.0	9

#	Article	IF	CITATIONS
289	Analysis of plasma termination in the JET hybrid scenario. Nuclear Fusion, 2018, 58, 076027.	1.6	9
290	The software and hardware architecture of the real-time protection of in-vessel components in JET-ILW. Nuclear Fusion, 2019, 59, 076016.	1.6	9
291	Full-orbit and drift calculations of fusion product losses due to explosive fishbones on JET. Nuclear Fusion, 2019, 59, 016004.	1.6	9
292	Measurements of 2D poloidal plasma profiles and fluctuations in ECRH plasmas using the heavy ion beam probe system in the TJ-II stellarator. Physics of Plasmas, 2020, 27, .	0.7	9
293	Experimental observation of the geodesic acoustic frequency limit for the NBI-driven Alfvén eigenmodes in TJ-II. Physics of Plasmas, 2021, 28, 072510.	0.7	9
294	Radial electric fields and confinement in the TJ-II stellarator. European Physical Journal D, 2005, 55, 317-339.	0.4	8
295	Turbulence studies by fast camera imaging experiments in the TJII stellarator. Journal of Nuclear Materials, 2009, 390-391, 457-460.	1.3	8
296	Fast visible imaging of ELM-wall interactions on JET. Journal of Nuclear Materials, 2009, 390-391, 797-800.	1.3	8
297	The Visible Intensified Cameras for Plasma Imaging in the TJâ€II Stellarator. Contributions To Plasma Physics, 2011, 51, 742-753.	0.5	8
298	Plasma isotopic changeover experiments in JET under carbon and ITER-like wall conditions. Nuclear Fusion, 2015, 55, 043021.	1.6	8
299	Characterization of a diamond detector to be used as neutron yield monitor during the in-vessel calibration of JET neutron detectors in preparation of the DT experiment. Fusion Engineering and Design, 2016, 106, 93-98.	1.0	8
300	On the mechanisms governing gas penetration into a tokamak plasma during a massive gas injection. Nuclear Fusion, 2017, 57, 016027.	1.6	8
301	The near infrared imaging system for the real-time protection of the JET ITER-like wall. Physica Scripta, 2017, T170, 014027.	1.2	8
302	Characterization of a compact LaBr ₃ (Ce) detector with Silicon photomultipliers at high 14 MeV neutron fluxes. Journal of Instrumentation, 2017, 12, C10007-C10007.	0.5	8
303	Detection and investigation of chirping Alfvén eigenmodes with heavy ion beam probe in the TJ-II stellarator. Nuclear Fusion, 2018, 58, 082019.	1.6	8
304	Analysis of possible improvement of the plasma performance in JET due to the inward spatial channelling of fast-ion energy. Nuclear Fusion, 2018, 58, 076012.	1.6	8
305	On the universality of power laws for tokamak plasma predictions. Plasma Physics and Controlled Fusion, 2018, 60, 025028.	0.9	8
306	On the role of finite grid extent in SOLPS-ITER edge plasma simulations for JET H-mode discharges with metallic wall. Nuclear Materials and Energy, 2018, 17, 174-181.	0.6	8

#	Article	IF	CITATIONS
307	Neutron emission spectroscopy of D plasmas at JET with a compact liquid scintillating neutron spectrometer. Review of Scientific Instruments, 2018, 89, 101113.	0.6	8
308	A locked mode indicator for disruption prediction on JET and ASDEX upgrade. Fusion Engineering and Design, 2019, 138, 254-266.	1.0	8
309	Simulation of neutron emission in neutral beam injection heated plasmas with the real-time code RABBIT. Nuclear Fusion, 2019, 59, 086002.	1.6	8
310	An assessment of nitrogen concentrations from spectroscopic measurements in the JET and ASDEX upgrade divertor. Nuclear Materials and Energy, 2019, 18, 147-152.	0.6	8
311	2D distributions of potential and density mean-values and oscillations in the ECRH and NBI plasmas at the TJ-II stellarator. Plasma Physics and Controlled Fusion, 2022, 64, 054009.	0.9	8
312	Computer simulations of the behaviour of the partial charge collection model in thick HgI2 γ-detectors. Nuclear Instruments and Methods in Physics Research, Section A: Accelerators, Spectrometers, Detectors and Associated Equipment, 1991, 302, 91-104.	0.7	7
313	Study of the plasma potential evolution during ECRH in the T-10 tokamak and TJ-II stellarator. European Physical Journal D, 2005, 55, 1569-1578.	0.4	7
314	Fast visible camera installation and operation in JET. AIP Conference Proceedings, 2008, , .	0.3	7
315	On the link between parallel flows, turbulence and electric fields in the edge of the TJ-II stellarator. Europhysics Letters, 2009, 85, 25002.	0.7	7
316	Turbulent transport analysis of JET H-mode and hybrid plasmas using QuaLiKiz and Trapped Gyro Landau Fluid. Plasma Physics and Controlled Fusion, 2015, 57, 035003.	0.9	7
317	Edge profile analysis of Joint European Torus (JET) Thomson scattering data: Quantifying the systematic error due to edge localised mode synchronisation. Review of Scientific Instruments, 2016, 87, 013507.	0.6	7
318	Comparison of dust transport modelling codes in a tokamak plasma. Physics of Plasmas, 2016, 23, 102506.	0.7	7
319	Real-time control of ELM and sawtooth frequencies: similarities and differences. Nuclear Fusion, 2016, 56, 016008.	1.6	7
320	JET experience on managing radioactive waste and implications for ITER. Fusion Engineering and Design, 2016, 109-111, 979-985.	1.0	7
321	Advances in understanding and utilising ELM control in JET. Plasma Physics and Controlled Fusion, 2016, 58, 014017.	0.9	7
322	Commissioning and first results of the reinstated JET ICRF ILA. Fusion Engineering and Design, 2017, 123, 285-288.	1.0	7
323	The preparation of the Shutdown Dose Rate experiment for the next JET Deuterium-Tritium campaign. Fusion Engineering and Design, 2017, 123, 1039-1043.	1.0	7
324	Expanding the role of impurity spectroscopy for investigating the physics of high-Z dissipative divertors. Nuclear Materials and Energy, 2017, 12, 91-99.	0.6	7

#	Article	IF	CITATIONS
325	Main chamber wall plasma loads in JET-ITER-like wall at high radiated fraction. Nuclear Materials and Energy, 2017, 12, 234-240.	0.6	7
326	Real time control developments at JET in preparation for deuterium-tritium operation. Fusion Engineering and Design, 2017, 123, 535-540.	1.0	7
327	Synthetic neutron camera and spectrometer in JET based on AFSI-ASCOT simulations. Journal of Instrumentation, 2017, 12, C09010-C09010.	0.5	7
328	Detection of Causal Relations in Time Series Affected by Noise in Tokamaks Using Geodesic Distance on Gaussian Manifolds. Entropy, 2017, 19, 569.	1.1	7
329	Testing of tritium breeder blanket activation foil spectrometer during JET operations. Fusion Engineering and Design, 2018, 136, 258-264.	1.0	7
330	MHD spectroscopy of JET plasmas with pellets via Alfvén eigenmodes. Nuclear Fusion, 2018, 58, 082008.	1.6	7
331	JET diagnostic enhancements testing and commissioning in preparation for DT scientific campaigns. Review of Scientific Instruments, 2018, 89, 10K119.	0.6	7
332	TLD calibration for neutron fluence measurements at JET fusion facility. Nuclear Instruments and Methods in Physics Research, Section A: Accelerators, Spectrometers, Detectors and Associated Equipment, 2018, 904, 202-213.	0.7	7
333	Modelling of the effect of ELMs on fuel retention at the bulk W divertor of JET. Nuclear Materials and Energy, 2019, 19, 397-402.	0.6	7
334	Comparison of the structure of the plasma-facing surface and tritium accumulation in beryllium tiles from JET ILW campaigns 2011–2012 and 2013–2014. Nuclear Materials and Energy, 2019, 19, 131-136.	0.6	7
335	Gyrokinetic simulations of toroidal Alfvén eigenmodes excited by energetic ions and external antennas on the Joint European Torus. Nuclear Fusion, 2019, 59, 026008.	1.6	7
336	Improved neutron activation dosimetry for fusion. Fusion Engineering and Design, 2019, 139, 109-114.	1.0	7
337	Improvements in the treatment of signals used for plasma diagnostics. IEEE Transactions on Nuclear Science, 1996, 43, 229.	1.2	6
338	Spontaneous edge E × B sheared flow development studies in the TJ-II stellarator. European Physical Journal D, 2005, 55, 1579-1587.	0.4	6
339	Two-Dimensional Turbulence Analysis Using High-Speed Visible Imaging in TJ-II Edge Plasmas. Fusion Science and Technology, 2006, 50, 301-306.	0.6	6
340	Comparative analysis of core heat transport of JET high density H-mode plasmas in carbon wall and ITER-like wall. Plasma Physics and Controlled Fusion, 2015, 57, 065002.	0.9	6
341	Integrated core–SOL–divertor modelling for ITER including impurity: effect of tungsten on fusion performance in H-mode and hybrid scenario. Nuclear Fusion, 2015, 55, 053032.	1.6	6
342	Simulating the nitrogen migration in Be/W tokamaks with WallDYN. Physica Scripta, 2016, T167, 014079.	1.2	6

#	Article	IF	CITATIONS
343	ITER-like antenna capacitors voltage probes: Circuit/electromagnetic calculations and calibrations. Review of Scientific Instruments, 2016, 87, 104705.	0.6	6
344	Evaluation of reconstruction errors and identification of artefacts for JET gamma and neutron tomography. Review of Scientific Instruments, 2016, 87, 013502.	0.6	6
345	COREDIV and SOLPS Numerical Simulations of the Nitrogen Seeded JET ILW Lâ€mode Discharges. Contributions To Plasma Physics, 2016, 56, 760-765.	0.5	6
346	Effect of PFC Recycling Conditions on JET Pedestal Density. Contributions To Plasma Physics, 2016, 56, 754-759.	0.5	6
347	Global optimization driven by genetic algorithms for disruption predictors based on APODIS architecture. Fusion Engineering and Design, 2016, 112, 1014-1018.	1.0	6
348	Investigation on the erosion/deposition processes in the ITER-like wall divertor at JET using glow discharge optical emission spectrometry technique. Physica Scripta, 2016, T167, 014049.	1.2	6
349	Impact of the JET ITER-like wall on H-mode plasma fueling. Nuclear Fusion, 2017, 57, 066024.	1.6	6
350	The effect of lower hybrid waves on JET plasma rotation. Nuclear Fusion, 2017, 57, 034002.	1.6	6
351	Evaluation of the plasma hydrogen isotope content by residual gas analysis at JET and AUG. Physica Scripta, 2017, T170, 014021.	1.2	6
352	Quartz micro-balance results of pulse-resolved erosion/deposition in the JET-ILW divertor. Nuclear Materials and Energy, 2017, 12, 478-482.	0.6	6
353	Analysis of activation and damage of ITER material samples expected from DD/DT campaign at JET. Fusion Engineering and Design, 2017, 125, 307-313.	1.0	6
354	Impurity re-distribution in the corner regions of the JET divertor. Physica Scripta, 2017, T170, 014060.	1.2	6
355	Self-consistent coupling of DSMC method and SOLPS code for modeling tokamak particle exhaust. Nuclear Fusion, 2017, 57, 066037.	1.6	6
356	An improved model for the accurate calculation of parallel heat fluxes at the JET bulk tungsten outer divertor. Nuclear Fusion, 2018, 58, 106034.	1.6	6
357	Geodesic acoustic mode evolution in L-mode approaching the L–H transition on JET. Plasma Physics and Controlled Fusion, 2019, 61, 075007.	0.9	6
358	Tritium analysis of divertor tiles used in JET ITER-like wall campaigns by means of <i>β</i> -ray induced x-ray spectrometry. Physica Scripta, 2017, T170, 014014.	1.2	6
359	Time-resolved deposition in the remote region of the JET-ILW divertor: measurements and modelling. Physica Scripta, 2017, T170, 014059.	1.2	6
360	Dynamics of flows and confinement in the TJ-II stellarator. Nuclear Fusion, 2013, 53, 104016.	1.6	5

#	Article	IF	CITATIONS
361	The merits of ion cyclotron resonance heating schemes for sawtooth control in tokamak plasmas. Journal of Plasma Physics, 2015, 81, .	0.7	5
362	Core fusion power gain and alpha heating in JET, TFTR, and ITER. Nuclear Fusion, 2016, 56, 056002.	1.6	5
363	Neutronic analysis of JET external neutron monitor response. Fusion Engineering and Design, 2016, 109-111, 99-103.	1.0	5
364	The non-thermal origin of the tokamak low-density stability limit. Nuclear Fusion, 2016, 56, 056010.	1.6	5
365	Plasma turbulence measured with fast frequency swept reflectometry in JET H-mode plasmas. Nuclear Fusion, 2016, 56, 126019.	1.6	5
366	Hybrid cancellation of ripple disturbances arising in AC/DC converters. Automatica, 2017, 77, 344-352.	3.0	5
367	Ceneration of the neutron response function of an NE213 scintillator for fusion applications. Nuclear Instruments and Methods in Physics Research, Section A: Accelerators, Spectrometers, Detectors and Associated Equipment, 2017, 866, 222-229.	0.7	5
368	Development of MPPC-based detectors for high count rate DT campaigns at JET. Fusion Engineering and Design, 2017, 123, 940-944.	1.0	5
369	Characterisation of neutron generators and monitoring detectors for the in-vessel calibration of JET. Fusion Engineering and Design, 2018, 136, 233-238.	1.0	5
370	Plasma-wall interaction on the divertor tiles of JET ITER-like wall from the viewpoint of micro/nanoscopic observations. Fusion Engineering and Design, 2018, 136, 199-204.	1.0	5
371	ICRH antennaS-matrix measurements and plasma coupling characterisation at JET. Nuclear Fusion, 2018, 58, 046012.	1.6	5
372	Shutdown dose rate measurements after the 2016 Deuterium-Deuterium campaign at JET. Fusion Engineering and Design, 2018, 136, 1348-1353.	1.0	5
373	Application of the Denovo Discrete Ordinates Radiation Transport Code to Large-Scale Fusion Neutronics. Fusion Science and Technology, 2018, 74, 303-314.	0.6	5
374	Shutdown dose rate neutronics experiment during high performances DD operations at JET. Fusion Engineering and Design, 2018, 136, 1545-1549.	1.0	5
375	Preparation for commissioning of materials detritiation facility at Culham Science Centre. Fusion Engineering and Design, 2018, 136, 1391-1395.	1.0	5
376	Scaling of the geodesic acoustic mode amplitude on JET. Plasma Physics and Controlled Fusion, 2018, 60, 085006.	0.9	5
377	RF sheath modeling of experimentally observed plasma surface interactions with the JET ITER-Like Antenna. Nuclear Materials and Energy, 2019, 19, 324-329.	0.6	5
378	Approximate analytic expressions using Stokes model for tokamak polarimetry and their range of validity. Plasma Physics and Controlled Fusion, 2019, 61, 055008.	0.9	5

#	Article	IF	CITATIONS
379	Gamma ray imaging using coded aperture masks: a computer simulation approach. Applied Optics, 1991, 30, 549.	2.1	4
380	Design of a modified uniform redundant-array mask for portable gamma cameras. Applied Optics, 1992, 31, 4742.	2.1	4
381	The global build-up to intrinsic edge localized mode bursts seen in divertor full flux loops in JET. Physics of Plasmas, 2015, 22, .	0.7	4
382	Conceptual Design of the Mechanical Tritium Pumping System for JET DTE2. Fusion Science and Technology, 2015, 68, 630-634.	0.6	4
383	Scaling of the frequencies of the type one edge localized modes and their effect on the tungsten source in JET ITER-like wall. Plasma Physics and Controlled Fusion, 2016, 58, 125014.	0.9	4
384	A prototype fully digital data acquisition system upgrade for the TOFOR neutron spectrometer at JET. Nuclear Instruments and Methods in Physics Research, Section A: Accelerators, Spectrometers, Detectors and Associated Equipment, 2016, 833, 94-104.	0.7	4
385	Stabilization of sawteeth with third harmonic deuterium ICRF-accelerated beam in JET plasmas. Physics of Plasmas, 2016, 23, 012505.	0.7	4
386	Risk Mitigation for ITER by a Prolonged and Joint International Operation of JET. Journal of Fusion Energy, 2016, 35, 85-93.	0.5	4
387	Calculation of the profile-dependent neutron backscatter matrix for the JET neutron camera system. Fusion Engineering and Design, 2017, 123, 865-868.	1.0	4
388	CeBr3–based detector for gamma-ray spectrometer upgrade at JET. Fusion Engineering and Design, 2017, 123, 986-989.	1.0	4
389	Determining the prediction limits of models and classifiers with applications for disruption prediction in JET. Nuclear Fusion, 2017, 57, 016024.	1.6	4
390	Be ITER-like wall at the JET tokamak under plasma. Physica Scripta, 2017, T170, 014049.	1.2	4
391	Synthetic NPA diagnostic for energetic particles in JET plasmas. Journal of Instrumentation, 2017, 12, C11025-C11025.	0.5	4
392	Control and data acquisition software upgrade for JET gamma-ray diagnostics. Fusion Engineering and Design, 2018, 128, 117-121.	1.0	4
393	Application of the VUV and the soft x-ray systems on JET for the study of intrinsic impurity behavior in neon seeded hybrid discharges. Review of Scientific Instruments, 2018, 89, 10D131.	0.6	4
394	Inter-ELM evolution of the edge current density in JET-ILW type I ELMy H-mode plasmas. Plasma Physics and Controlled Fusion, 2018, 60, 085003.	0.9	4
395	On a fusion born triton effect in JET deuterium discharges with H-minority ion cyclotron range of frequencies heating. Nuclear Fusion, 2019, 59, 064001.	1.6	4
396	Operation of a multiple cell array detector in plasma experiments with a heavy ion beam diagnostic. Review of Scientific Instruments, 2004, 75, 3511-3513.	0.6	3

#	Article	IF	CITATIONS
397	Quasi-coherent Oscillations in the TJ-II Stellarator. AIP Conference Proceedings, 2006, , .	0.3	3
398	Observation of Filamentary Structures on the Boundary Region of the LHD Stellarator. Contributions To Plasma Physics, 2011, 51, 92-98.	0.5	3
399	Robust regression with CUDA and its application to plasma reflectometry. Review of Scientific Instruments, 2015, 86, 113507.	0.6	3
400	Free boundary equilibrium in 3D tokamaks with toroidal rotation. Nuclear Fusion, 2015, 55, 063032.	1.6	3
401	Comparative gyrokinetic analysis of JET baseline H-mode core plasmas with carbon wall and ITER-like wall. Plasma Physics and Controlled Fusion, 2016, 58, 045021.	0.9	3
402	A classification scheme for edge-localized modes based on their probability distributions. Review of Scientific Instruments, 2016, 87, 11D404.	0.6	3
403	Numerical calculations of non-inductive current driven by microwaves in JET. Plasma Physics and Controlled Fusion, 2016, 58, 125001.	0.9	3
404	JET Tokamak, preparation of a safety case for tritium operations. Fusion Engineering and Design, 2016, 109-111, 1308-1312.	1.0	3
405	Kinematic background discrimination methods using a fully digital data acquisition system for TOFOR. Nuclear Instruments and Methods in Physics Research, Section A: Accelerators, Spectrometers, Detectors and Associated Equipment, 2016, 838, 82-88.	0.7	3
406	Modelling of the JET DT Experiments in Carbon and ITER-like Wall Configurations. Contributions To Plasma Physics, 2016, 56, 766-771.	0.5	3
407	Correlation analysis for energy losses, waiting times and durations of type I edge-localized modes in the Joint European Torus. Nuclear Fusion, 2017, 57, 036026.	1.6	3
408	The global build-up to intrinsic ELM bursts and comparison with pellet triggered ELMs seen in JET. Nuclear Fusion, 2017, 57, 022017.	1.6	3
409	A 3D electromagnetic model of the iron core in JET. Fusion Engineering and Design, 2017, 123, 527-531.	1.0	3
410	EDGE2D-EIRENE simulations of the impact of poloidal flux expansion on the radiative divertor performance in JET. Nuclear Materials and Energy, 2017, 12, 786-790.	0.6	3
411	Intra-ELM tungsten sputtering in JET ITER-like wall: analytical studies of Be impurity and ELM type influence. Physica Scripta, 2017, T170, 014065.	1.2	3
412	Evidence of9Be  +  pnuclear reactions during 2ωCHand hydrogen minority ICRH in JET-ILW hy deuterium plasmas. Nuclear Fusion, 2018, 58, 026033.	vdrogen a	nd 3
413	Escaping alpha-particle monitor for burning plasmas. Nuclear Fusion, 2018, 58, 082009.	1.6	3
414	Nonlinear dynamic analysis of Dαsignals for type I edge localized modes characterization on JET with a	0.9	3

414 carbon wall. Plasma Physics and Controlled Fusion, 2018, 60, 025010.

#	Article	IF	CITATIONS
415	Heat flux analysis of Type-I ELM impact on a sloped, protruding surface in the JET bulk tungsten divertor. Nuclear Materials and Energy, 2018, 17, 182-187.	0.6	3
416	OVERVIEW OF NEUTRON MEASUREMENTS IN JET FUSION DEVICE. Radiation Protection Dosimetry, 2018, 180, 102-108.	0.4	3
417	Activation material selection for multiple foil activation detectors in JET TT campaign. Fusion Engineering and Design, 2018, 136, 988-992.	1.0	3
418	Alpha heating, isotopic mass, and fast ion effects in deuterium–tritium experiments. Nuclear Fusion, 2018, 58, 096011.	1.6	3
419	Modelling of beam-driven Alfvén modes in TJ-II plasmas. Nuclear Fusion, 2019, 59, 056002.	1.6	3
420	Impact of fast ions on density peaking in JET: fluid and gyrokinetic modeling. Plasma Physics and Controlled Fusion, 2019, 61, 075008.	0.9	3
421	Radial variation of heat transport in L-mode JET discharges. Nuclear Fusion, 2019, 59, 056006.	1.6	3
422	Analysis of the outer divertor hot spot activity in the protection video camera recordings at JET. Fusion Engineering and Design, 2019, 139, 115-123.	1.0	3
423	Topology of 2-D turbulent structures based on intermittence in the TJ-II stellarator. Nuclear Fusion, 0, , .	1.6	3
424	Sailing the Prestige out to sea. An independent analysis. Scientia Marina, 2011, 75, 533-548.	0.3	3
425	Plasma Electric Potential Evolution at the Core and Edge of the TJ-II Stellarator and T-10 Tokamak. AIP Conference Proceedings, 2006, , .	0.3	2
426	Evaluation of the Faraday angle by numerical methods and comparison with the Tore Supra and JET polarimeter electronics. Review of Scientific Instruments, 2011, 82, 043502.	0.6	2
427	Dust observation with a visible fast camera in the TJ-II stellarator. Plasma Physics and Controlled Fusion, 2013, 55, 065001.	0.9	2
428	Studies of the non-axisymmetric plasma boundary displacement in JET in presence of externally applied magnetic field. Plasma Physics and Controlled Fusion, 2015, 57, 104003.	0.9	2
429	Ion temperature and toroidal rotation in JET's low torque plasmas. Review of Scientific Instruments, 2016, 87, 11E557.	0.6	2
430	A generalized Abel inversion method for gamma-ray imaging of thermonuclear plasmas. Journal of Instrumentation, 2016, 11, C03001-C03001.	0.5	2
431	Thermo-mechanical properties of W/Mo markers coatings deposited on bulk W. Physica Scripta, 2016, T167, 014028.	1.2	2
432	Modelling of plasma-edge and plasma–wall interaction physics at JET with the metallic first-wall. Physica Scripta, 2016, T167, 014078.	1.2	2

#	Article	IF	CITATIONS
433	Towards self-consistent plasma modelisation in presence of neoclassical tearing mode and sawteeth: effects on transport coefficients. Plasma Physics and Controlled Fusion, 2017, 59, 125012.	0.9	2
434	Gyrokinetic simulations of particle transport in pellet fuelled JET discharges. Plasma Physics and Controlled Fusion, 2017, 59, 105005.	0.9	2
435	Dynamic power balance analysis in JET. Physica Scripta, 2017, T170, 014035.	1.2	2
436	Real-time implementation with FPGA-based DAQ system of a probabilistic disruption predictor from scratch. Fusion Engineering and Design, 2018, 129, 179-182.	1.0	2
437	Control and data acquisition system for the multiple cell array detector of the TJ-II heavy ion beam diagnostic. Fusion Engineering and Design, 2006, 81, 1885-1889.	1.0	1
438	ITER CODAC interface for the visible and infra-red wide angle viewing cameras. Fusion Engineering and Design, 2009, 84, 1412-1415.	1.0	1
439	X-ray micro-laminography for the <i>ex situ</i> analysis of W-CFC samples retrieved from JET ITER-like wall. Physica Scripta, 2016, T167, 014050.	1.2	1
440	Thermal analysis of protruding surfaces in the JET divertor. Nuclear Fusion, 2017, 57, 066009.	1.6	1
441	Classification of ELM types in Joint European Torus based on global plasma parameters using discriminant analysis. Fusion Engineering and Design, 2017, 123, 717-721.	1.0	1
442	Divertor currents optimization procedure for JET-ILW high flux expansion experiments. Fusion Engineering and Design, 2018, 129, 115-119.	1.0	1
443	Modelling of JET DT experiments in ILW configurations. Contributions To Plasma Physics, 2018, 58, 739-745.	0.5	1
444	Activation Inventories after Exposure to DD/DT Neutrons in Safety Analysis of Nuclear Fusion Installations. Radiation Protection Dosimetry, 2018, 180, 125-128.	0.4	1
445	Energetic ion losses †channeling' mechanism and strategy for mitigation. Plasma Physics and Controlled Fusion, 2019, 61, 084008.	0.9	1
446	Population modelling of the He II energy levels in tokamak plasmas: I. Collisional excitation model. Journal of Physics B: Atomic, Molecular and Optical Physics, 2019, 52, 045001.	0.6	1
447	Micro ion beam analysis for the erosion of beryllium marker tiles in a tokamak limiter. Nuclear Instruments & Methods in Physics Research B, 2019, 450, 200-204.	0.6	1
448	On determining the prediction limits of mathematical models for time series. Journal of Instrumentation, 2016, 11, C07013-C07013.	0.5	1
449	Classification of JET Neutron and Gamma Emissivity Profiles. Journal of Instrumentation, 2016, 11, C05021-C05021.	0.5	0
450	MHD marking using the MSE polarimeter optics in ILW JET plasmas. Review of Scientific Instruments, 2016, 87, 11E556.	0.6	0

#	Article	IF	CITATIONS
451	Characteristics of pre-ELM structures during ELM control experiment on JET withn  =  2 magnet perturbations. Nuclear Fusion, 2016, 56, 092011.	ic 1.6	0
452	First observation of the depolarization of Thomson scattering radiation by a fusion plasma. Nuclear Fusion, 2018, 58, 044003.	1.6	0
453	Propagating transport-code input parameter uncertainties with deterministic sampling. Plasma Physics and Controlled Fusion, 2018, 60, 125010.	0.9	0